Received: 9 January 2020 | Revised: 11 June 2020 | Accepted: 11 June 2020

DOI: 10.1096/fj.201902515RR

RESEARCH ARTICLE

THE FASEB JOURNAL

Bivalent engagement of endothelial surface antigens is critical to prolonged surface targeting and protein delivery in vivo

R. Yu. Kiseleva[1] | P. G. Glassman[1] | K. M. LeForte[1] | L. R. Walsh[1] | C. H. Villa[1] | V. V. Shuvaev[1] | J. W. Myerson[1] | P. A. Aprelev[1] | O. A. Marcos-Contreras[1] | V. R. Muzykantov[1] | C. F. Greineder[2]

[1]Department of Pharmacology, The Perelman School of Medicine, University of Pennsylvania, Philadelphia, PA, USA

[2]Department of Emergency Medicine and Pharmacology, University of Michigan, Ann Arbor, MI, USA

Correspondence
C. F. Greineder, Department of Emergency Medicine and Pharmacology, University of Michigan, North Campus Research Complex, B10-154A, Ann Arbor, MI, USA.
Email: coling@med.umich.edu

Funding information
HHS | NIH | National Heart, Lung, and Blood Institute (NHLBI), Grant/Award Number: K08-HL130430, RO1 HL125462 and RO1 HL128398

Abstract

Targeted drug delivery to the endothelium has the potential to generate localized therapeutic effects at the blood-tissue interface. For some therapeutic cargoes, it is essential to maintain contact with the bloodstream to exert protective effects. The pharmacokinetics (PK) of endothelial surface-targeted affinity ligands and biotherapeutic cargo remain a largely unexplored area, despite obvious translational implications for this strategy. To bridge this gap, we site-specifically radiolabeled mono- (scFv) and bivalent (mAb) affinity ligands specific for the endothelial cell adhesion molecules, PECAM-1 (CD31) and ICAM-1 (CD54). Radiotracing revealed similar lung biodistribution at 30 minutes post-injection (79.3% ± 4.2% vs 80.4% ± 10.6% ID/g for αICAM and 58.9% ± 3.6% ID/g vs. 47.7% ± 5.8% ID/g for αPECAM mAb vs. scFv), but marked differences in organ residence time, with antibodies demonstrating an order of magnitude greater area under the lung concentration vs. time curve (AUC_{inf} 1698 ± 352 vs. 53.3 ± 7.9 ID/g*hrs for αICAM and 1023 ± 507 vs. 114 ± 37 ID/g*hrs for αPECAM mAb vs scFv). A physiologically based pharmacokinetic model, fit to and validated using these data, indicated contributions from both superior binding characteristics and prolonged circulation time supporting multiple binding-detachment cycles. We tested the ability of each affinity ligand to deliver a prototypical surface cargo, thrombomodulin (TM), using one-to-one protein conjugates. Bivalent mAb-TM was superior to monovalent scFv-TM in both pulmonary targeting and lung residence time (AUC_{inf} 141 ± 3.2 vs 12.4 ± 4.2 ID/g*hrs for ICAM and 188 ± 90 vs 34.7 ± 19.9 ID/g*hrs for PECAM), despite having similar blood PK, indicating that binding strength is more important parameter than the kinetics of binding. To maximize bivalent target engagement, we synthesized an oriented, end-to-end anti-ICAM mAb-TM conjugate and found that this therapeutic had the best lung residence time (AUC_{inf} 253 ± 18 ID/g*hrs) of all TM

Abbreviations: AUC, area under the lung concentration vs. time curve; ICAM, intercellular cell adhesion molecule-1; ID/g, injected dose per gram of tissue; Kd, equilibrium affinity; Kon, association constant; Koff, dissociation constant; PECAM, platelet endothelial cell adhesion molecule-1; PK, pharmacokinetics; scFv, single-chain variable fragment; SPR, surface plasmon resonance; TM, thrombomodulin.

modalities. These observations have implications not only for the delivery of TM, but also potentially all therapeutics targeted to the endothelial surface.

KEYWORDS

cell surface, endothelium, ICAM-1, PECAM-1, targeted drug delivery, thrombomodulin

The vascular endothelium is a critical site for therapeutic action in a variety of human diseases,[1] in large part because of the numerous physiologic functions of the endothelial monolayer and the consequences of dysfunction and/or injury to these pleiotropic cells.[2] The concept of targeting drugs or drug carriers to endothelial surface molecules has been advanced by a number of laboratories over the past several decades, but most applications have focused on either transcytosis (ie, using affinity ligands to induce transport across the endothelium) or delivery of therapeutics into endothelial cells, with the goal of modulating intracellular signaling pathways and/or gene expression. Less attention has been paid to the possibility of targeting the endothelial surface, where integral membrane proteins project into the bloodstream and modulate coagulation, fibrinolysis, barrier function, and the adhesion of circulating blood cells. Therapeutic delivery of recombinant biotherapeutics to the luminal membrane has the potential to modulate these critical processes, but only if surface localization is maintained. From a drug delivery standpoint, these applications require prolonged target engagement while avoiding endocytosis, which effectively removes the therapeutic from its necessary site of action.

Surface delivery precludes the use of a number of commonly cited endothelial targets–membrane proteins like transferrin receptor-1, angiotensin-converting enzyme, aminopeptidase-P, and the plasmalemma-vesicle associated protein (PLVAP, or PV-1)–due to their rapid internalization in response to the binding of affinity ligands.[3-8] In contrast, the Platelet Endothelial Cell Adhesion Molecule-1 (PECAM-1, or CD31) is highly expressed in nearly every vascular bed, predominantly endothelial (~10^6 copies/endothelial cell vs only ~5×10^3/platelet and 5×10^4/leukocyte), poorly internalized, and minimally affected by disease states, making it a prime choice for endothelial surface delivery.[9,10] The Intercellular Adhesion Molecule-1 (ICAM-1, or CD54), while inducible and less specific for endothelial cells, is also highly expressed on the pulmonary vasculature and has been repeatedly utilized as a target for surface delivery due to its low rates of endocytosis and the rapid recycling of internalized cargo back to the surface.[11-14] With this in mind, our group developed monovalent affinity ligands to PECAM-1 and ICAM-1 and fused them to therapeutic proteins like plasminogen activators, thrombomodulin (TM), and the endothelial protein C receptor (EPCR).[15] In addition to minimizing internalization, the fusion protein approach is meant to ensure consistent orientation of affinity ligand and cargo protein and offer straightforward translation to industrial development and preclinical testing.[16]

The CAM-targeted scFv-fusion protein paradigm has found consistent success over the past decade.[16] scFv/TM and scFv/ECPR, in particular, have been shown to boost the endogenous protein C pathway and re-establish the anticoagulant phenotype of the endothelium following inflammatory activation/dysfunction.[14,17,18] Our group recently demonstrated this in a human whole blood, microfluidic model of inflammatory thrombosis, in which an anti-ICAM (αICAM) scFv/TM fusion protein effectively eliminated fibrin deposition, outperforming other anticoagulant biotherapeutics like hirudin, soluble TM, and tissue factor blocking antibody.[19] CAM-targeted scFv fusion proteins have also achieved some degree of success in vivo, reducing leukocyte accumulation and barrier dysfunction in mouse models of inflammatory, ischemic, and oxidative lung injury.[14,17,18]

At the same time, comprehensive understanding of in vivo behavior and translation to large animal studies has been limited by a number of unanticipated difficulties. First and foremost, assessment of PK has been hampered by partial, or in some cases, complete loss of affinity for the target antigen following radiolabeling. As a result, biodistribution studies have been inconsistent and those experiments that have successfully demonstrated endothelial targeting have revealed a lower level of tissue (eg, lung) uptake than anticipated based on studies of parental antibodies.[14,17,18] While isolated scFv might be expected to underperform, due to small size and corresponding renal clearance, fusion to large proteins like TM had been expected to improve PK substantially.

Here, we seek to address these shortcomings by taking advantage of recently reported techniques for site-specific modification, which allow C-terminal functionalization and bioconjugation to protein cargo without appreciable loss of binding to target antigens.[20] We demonstrate site-specific radiolabeling of ICAM- and PECAM-targeted scFv and make two surprising observations: 1. mAb and scFv have similar levels of endothelial targeting at early time points, and 2. mAb are far superior in maintaining surface localization and organ biodistribution over time. We construct a physiologically based PK model and use it determine how affinity ligand characteristics contribute to differences in behavior in vivo. Finally, we compare the ability of scFv and mAb to deliver TM to the endothelial

surface and again find marked superiority of bivalent affinity ligands–in this case, without any apparent advantage in terms of blood PK. Ultimately, our observations motivate production of an oriented, end-to-end mAb-TM conjugate, which demonstrates the best endothelial surface targeting and organ residence time of any targeted TM modality. These results are of critical importance to future testing of endothelial targeted TM in animal models of human disease and have significant implications for all endothelial surface targeting applications.

2 | MATERIALS AND METHODS

2.1 | Reagents and cell lines

Unless otherwise indicated, cell culture reagents were purchased from Invitrogen (Carlsbad, CA, USA). [^{125}I]Na and [^{111}In] were purchased from PerkinElmer Life and Analytical Sciences (Waltham, MA, USA) and Nuclear Diagnostics Products (Cherry Hill, NJ), respectively. M2 anti-FLAG and anti-mouse secondary antibodies were from Sigma-Aldrich (St Louis, MO), as was bovine thrombin and hirudin. Protein C purified from human plasma was from Haematologic Technologies (Essex Junction, VT). APC substrate S-2366 was from Diapharma (West Chester, OH).

The wild-type REN mesothelioma cell line (REN-WT), and stably transfected variants expressing full-length mouse PECAM (REN-mPECAM) or ICAM (REN-mICAM) were maintained as previously described.[14,21] Immortalized murine endothelial cells, bEnd3, were obtained from ATCC (Manassas, VA) and grown in DMEM supplemented with 10% fetal bovine serum and antibiotic/antimycotic solution.[7]Immortalized mouse lung endothelial cells, PmT, were obtained from Applied Biological Materials Inc (ABM, Richmond, BC, Canada) and grown in PriGrow VI Medium (ABM, Richmond, BC, Canada).

2.2 | Protein production and purification

αPECAM (clone 390) and αICAM (clone YN1) mAb were produced and purified from hybridoma supernatants as previously described.[14,22] Sortagged scFv-LPETGG proteins–αPECAM (clone 390), αICAM (clone YN1), and an untargeted control (clone R6.5, binds human ICAM-1 with no cross-reactivity to mouse)–were produced as previously described in stably transfected *Drosophila* S2 cells or in the periplasmic space of *E coli* using the pBAD expression system (ThermoFisher Scientific).[20] Sortagged αICAM mAb-ss (YN1 mAb-LPETGG) was produced and purified from a CRISPR-Cas9-modified hybridoma, as previously described.[23] Finally, sortagged sTM-LPETGG was produced by inserting its cDNA between Bgl II and Sal I sites in the previously described vector, pMT/linker-LPETGG.[20] The vector was co-transfected with pCoBLAST in S2 cells and selected with blasticidin to generate a stable cell line. S2 cells were maintained in Schneider's medium (Thermo Fisher Scientific) and transitioned to Insect-Xpress (Lonza, Walkersville, MD) for protein production, as previously described.[14,20] All sortagged proteins also had a C-terminal triple FLAG and were purified using anti-FLAG (M2) affinity resin (Sigma-Aldrich), with the exception of αICAM mAb-ss, which was purified using protein G sepharose fast flow (GE Healthcare Life Sciences, Pittsburgh, PA). The purity of recombinant and hybridoma produced proteins was confirmed by SDS-PAGE and/or analytical SEC HPLC, using a Yarra 3 μm SEC-2000 LC Column 150 × 7.5 mm size exclusion column with a flow rate of 1.0 mL/min or a Yarra 3 μm SEC-2000 LC Column 300 × 4.6 mm size exclusion column with a flow rate of 0.35 mL/min. 0.1M sodium phosphate buffer at pH 7.0 was used as the mobile phase.

2.3 | Fluorescent and radioactive labeling of scFv and mAb

For flow cytometry experiments, αPECAM and αICAM mAb were labeled using AlexaFluor 647-NHS ester (Life Technologies, Carlsbad, CA) and purified using Zeba Spin Desalting Columns (Thermo Scientific, Waltham, MA). For radiotracing, antibodies directly radioiodinated using [^{125}I]NaI (PerkinElmer, Waltham, MA) in tubes pre-coated with 100 μg Pierce Iodination reagent, 1,3,4,6-tetrachloro-3α,6α-diphenyl-glycoluril (Thermo Fisher Scientific). Free iodine was removed using 0.5-mL Zeba Spin Desalting Column (Thermo Fisher Scientific). Radiochemical purity was > 95% by thin-layer chromatography (TLC) using a 75%:25% mixture of MeOH:Na-acetate pH 6.8 as the mobile phase. scFv-LPETGG were site-specifically radiolabeled with ^{111}In using SrtA-mediated transpeptidation. First, a peptide containing a radiometal chelating group (H_2N-GGGK-DOTA, Click Chemistry Reagents, San Diego, CA) was labeled with ^{111}In in metal-free 0.5M tetramethylammonium acetate (TMAA), pH 4.5, for 1 hour at 37°C. The pH was raised to 7.5 using 2M Tris buffer and the radiochemical purity (ie, % of radiometal bound to peptide) was confirmed to be > 95% using TLC, using 10mM Na-EDTA solution as mobile phase. Radiolabeled peptide was subsequently conjugated to scFv-LPETGG via SrtA-mediated transpeptidation, as described previously.[24] The reaction mixture was purified in two steps; His-tagged sortase (SrtA) was first removed using Ni-NTA resin (Qiagen, Germantown, MD), followed by desalting

of unreacted peptide using a 10DG column (Bio-Rad, Hercules, CA).

2.4 | Synthesis and purification of scFv-TM and mAb-TM conjugates

To synthesize scFv-sTM and mAb-sTM conjugates, sTM-LPETGG was first site-specifically modified with azide via sortase transpeptidation, as described previously.[20] Briefly, the protein (10 μM) was mixed with SrtA (2 μM) and a five-fold excess (50 μM) of a fluorescent peptide with a C-terminal azidolysine (GGGK[FAM]GSK-azide) in 1 mM $CaCl_2$ containing Tris-buffered saline (TBS), pH 7.0. The reaction was left at RT overnight and the product, sTM-azide, was purified in two steps: (1) Incubation with Ni-NTA resin to remove SrtA, and (2) centrifugation using a 30 kDa MWCO Amicon centrifugal filter (Millipore Sigma, Burlington MA) to remove unreacted peptide.

To enable conjugation to sTM-azide, each affinity ligand was modified with dibenzocyclooctyne (DBCO). αPECAM and αICAM mAb were reacted with DBCO-PEG_4-NHS ester (Jena Biosciences, Scottsdale, AZ) at a 1:5 ratio at pH 8.1 for 30 minutes at RT and quenched by adding 1M Tris-HCl. The reaction product, mAb-DBCO (NHS), was purified by centrifugal filtration using a 100 kDa MWCO Amicon.

scFv-LPETGG and the αICAM mAb-ss were, in contrast, site-specifically modified using a short peptide containing a C-terminal DBCO. This peptide was synthesized by reacting GGGK[FAM]GGSC (Pierce Custom Peptides, Rockford, IL) with sulfo DBCO-PEG_4-maleimide (Click Chemistry Tools, Scottsdale, AZ). The reaction was carried out for 2 hours at RT in degassed 0.1 M phosphate buffer, pH 7.0, with 10% DMSO. The DBCO peptide was separated from its components using a Sep Pak C18 Cartridge (Waters, Milford, MA) and its purity was verified on reverse phase HPLC. scFv-LPETGG and/or αICAM mAb-ss (10 μM) were then reacted with the DBCO peptide (50 μM) using SrtA (2 μM) in TBS with $CaCl_2$ (1 mM). In some cases, 150 mM NaCl and 10% glycerol were added to the reaction buffer to minimize aggregation of the reaction product. All reactions were purified using the same two-step procedure described above (Ni-NTA followed by centrifugal filtration to remove unreacted peptides).

Finally, scFv-sTM and mAb-TM conjugates were prepared by mixing sTM-azide with DBCO-modified affinity ligands. 1:5, 1:3, and 2:1 molar ratios of sTM:affinity ligand were used for scFv-TM, mAb-TM, and αICAM mAb-ss-TM conjugates, respectively. Reactions were left overnight at RT and 1:1 conjugates (ie, 1 sTM:1 affinity ligand) were purified by HPLC using a Yarra 5 μm SEC-3000 PREP, LC Column 300 × 21.2 mm with 0.1 M potassium phosphate buffer (pH 7.0) as a mobile phase and a flow rate of 5 mL/min. Radiolabeled conjugates were synthesized in an identical manner, incorporating radioiodinated sTM-azide. Labeling the cargo protein prior to conjugation ensured that neither the iodiation reaction nor the addition of the ^{125}I-moeity would impact affinity ligand function.

2.5 | Cell based radioimmunoassays and radio-internalization assays

Radioimmunoassays (RIAs) were performed on REN cells stably expressing the relevant CAMs as previously described.[11,25] Briefly, stably transfected cells and wild-type controls were grown to confluence in 96-strip-well microplates (Corning Life Sciences, Lowell, MA). To measure binding affinity, monolayers were incubated in quadruplicate for 2 Hr at 4°C with increasing concentrations of [^{125}I]- or [^{111}In]-labeled affinity ligands or protein conjugates, then washed five times with ice-cold assay buffer, prior to counting of cell-bound radioactivity (Wizard 2470, PerkinElmer). Radiointernalization assays were conducted as previously described.[11,26] Briefly, mAb and scFv were bound to cells at 4°C and then incubated at 37°C for various time points to allow endocytosis. Cells were washed three times with cold 50 mM glycine/100 mM NaCl to elute surface bound affinity ligands. This treatment has been shown previously not to damage cells [26] and three washes were confirmed as adequate to elute surface bound antibody, based on marked drop off in radioactive counts with each successive wash. Following surface elution, cells were lysed with 0.1% Triton X-100 and the radioactivity in cellular lysates and glycine eluates was measured. The percent internalization was calculated as % = [radioactivity in the lysate/(radioactivity in lysate + radioactivity in eluates)] × 100.

2.6 | Endothelial cell internalization studies

bEnd3 cells were grown to confluence on 1% gelatin coated glass coverslips. Cells were stimulated with 1 mg/mL LPS for 16 hours prior to incubation with mAb or scFv to induce ICAM-1 prior to binding of affinity ligands and internalization assays. Following incubation with mAb or scFv, cells were washed with ice-cold PBS and fixed with ice-cold 2% paraformaldehyde for 15 minutes. Cell surface bound protein was identified by incubating with Alexa Fluor 594-labeled secondary antibody for 1hr at room temperature (RT). Cells were then washed and permeabilized with 0.2% Triton X-100 for 15 minutes prior staining with Alexa Fluor 488 goat secondary for 1 hours at RT. Samples were washed, mounted using ProLong

Gold antifade reagent with DAPI (Invitrogen), and imaged using a Nikon Eclipse TE2000-U fluorescence microscope (Nikon, Tokyo, Japan). Image processing was carried out using Image-Pro Plus 4.5.1.27 (Media Cybernetics, Bethesda, MD, USA) as described previously.[27]

2.7 | Surface plasmon resonance (SPR)

Binding analysis was performed using a Biacore T200 from GE Healthcare (Uppsala, Sweden). SPR Sensor chips CMD 200L and the amine coupling kit containing 50 mM 2-(N-morpholino)ethanesulfonic acid/100 mM N-hydroxysuccinimide (MES/NHS), 1-ethyl-3-(3-dimethylaminopropyl) carbodiimide (EDC), 0.1 M Sodium Borate pH 9.0, and 1.0 M ethanolamine-HCl pH 8.5 were purchased from Xantec Bioanalytics GmbH, Germany. Antigen (recombinant soluble ICAM or PECAM, RnD Systems) was immobilized by injecting a 300 µL solution of 50 µg/mL protein at 15 µL/min for 9 minutes, followed by 1M ethanolamine pH 8.5 to block any activated groups on the gold chip. Binding and kinetic measurements were performed at 25°C and a flow rate of 30 µL/min. The gold chip was regenerated using 10 mM glycine-HCl, pH 2.5 to remove bound analyte. Biosensor data produced were evaluated with Biacore evaluation software 2.0 in a 1:1 global fit.

2.8 | In vitro APC generation by cell-bound conjugates

Measurement of protein C activation by cell bound TM conjugates was performed as previously described.[17] Briefly, cell monolayers were incubated with TM conjugates (1-50 nM), washed three times with assay buffer (20 mM Tris, 100 mM NaCl, 1 mM CaCl2, 0.1% (w/v) BSA, and pH 7.5) and incubated with 1 nM bovine thrombin and 100 nM human protein C for 20 minutes at room temperature. Thrombin was quenched with hirudin (50 U/mL), and APC was measured using Spectrozyme (OD 405 nm).[18]

2.9 | Animals

Animal studies were carried out in accordance with the *Guide for the Care and Use of Laboratory Animals* [National Institutes of Health, Bethesda, MD, USA (NIH)] under protocols approved by University of Pennsylvania Institutional Animal Care and Use Committee. Male C57BL/6 mice and TIE2-GFP transgenic mice, 6-8 weeks old, weighing 20-30 g (The Jackson Laboratory, Bar Harbor, ME, USA), were used for all biodistribution experiments and flow cytometry analysis.

2.10 | Flow cytometry for single cell suspensions prepared from mouse lungs

Flow cytometric analysis of disaggregated mouse lungs was performed as previously described.[28] In these experiments, TIE2-GFP transgenic mice and C57BL/6 controls (used to establish gates for GFP positivity) were used and 0.8mg/kg of AlexaFluor 647-tagged αPECAM or αICAM mAb were administered intravenously. After 30 minutes of circulation, animals were exsanguinated and lungs were perfused via the right ventricle with ~10 mL of cold PBS. A solution consisting of 5 U/mL dispase, 2.5 mg/mL collagenase type I, and 1 mg/mL of DNAse I was infused the tracheal catheter. Lungs were dissected with scissors and a scalpel and incubated in 2 mL of collagenase/dispase solution at 37°C for 45 minutes. One milliliter of fetal calf serum was added and the suspension was strained through 100 µm filters and centrifugation at 400 ×*g* for 5 minutes. Erythrocytes were lysed in 10 mL of cold ACK lysing buffer and the suspension was again strained, this time through a 40 µm filter, prior to centrifugation. Cell pellets were washed and fixed in 2% PFA in FACS buffer (2% fetal calf serum + 1 mM EDTA in PBS) for 10 minutes prior to staining with 1:500 dilution of PerCP-conjugated anti-CD45 antibody (Clone 30-F11, BD Biosciences) in FACS buffer. Cells were washed prior to analysis on a BD Accuri flow cytometer. Forward and side scatter data were gated to remove debris and exclude doublets. Single stain controls allowed automatic generation of compensation matrices in FCS Express software, applied uniformly to data from all samples.

2.11 | Measurement of blood and organ pharmacokinetics

Cocktails containing different amounts of unlabeled protein and a trace amount of radiolabeled protein (0.25 µg) were injected intravenously (via retro-orbital route of injection) into anesthetized mice. At the indicated time points, blood was drawn and mice were killed. Organs of interest were gently rinsed to remove blood, weighed, and the ^{125}I activity was measured in a gamma counter. Data are presented as the % of injected dose per gram of organ weight (% ID/g).

3 | RESULTS

3.1 | Intravenously injected αICAM and αPECAM mAb bind predominantly to endothelial cells in the lung

While a significant body of literature supports the utility of affinity targeting of PECAM-1 and ICAM-1 for endothelial

drug delivery,[13,14,16,19,24,27,29-33] much of this work has focused on multivalent polymeric, liposomal, and protein nanoparticles, and relatively few studies have investigated the cell types targeted in vivo.[28] To determine suitability for endothelial surface delivery, we first measured the distribution of intravenously injected, fluorescent PECAM and ICAM antibodies using flow cytometry of disaggregated organs. In this case, the lung was the primary organ of interest as it receives 100% of the cardiac output and is the first pass vascular bed for intravenously injected therapeutics. TIE2-GFP transgenic mice were employed to enable easy identification of endothelial cells and CD45 was used to identify leukocytes (Figures 1A and S1A). Fluorescent signal from injected antibodies was determined in GFP^+, $CD45^+$, and $GFP^-/CD45^-$ cells to quantitate localization to pulmonary endothelial cells, leukocytes, or other cell types (Figures S1B, and S1C).

As shown in Figure 1intravenous injection of 20μg (~0.8 mg/kg) of αPECAM or αICAM mAb resulted in antibody signal on nearly all pulmonary endothelial cells (97.7% ± 0.6% for αPECAM and 93.6% ± 0.4% for αICAM). In contrast, only 6.3% ± 0.1% and 36.6% ± 1.5% of leukocytes were positive for αPECAM and αICAM mAb, respectively (Figure 1B-E). Endothelial mean fluorescence intensity was similar for the two antibodies (Figure 1D), consistent with prior quantitative radiotracing experiments, which have shown similar pulmonary biodistribution of affinity ligands with these specificities.[30] Altogether, the data indicate that αPECAM and αICAM mAbs bind predominantly to endothelial cells in the lungs of intravenously injected mice and, at least from this standpoint, represent suitable targets for endothelial surface targeting.

3.2 | Bivalent vs. monovalent αPECAM and αICAM affinity ligands demonstrate similar initial pulmonary targeting but differ markedly in tissue PK

Having confirmed that endothelial cells are the primary target of PECAM and ICAM affinity ligands in vivo, our next step was to quantitatively characterize their biodistribution and PK, comparing full-length antibodies and their corresponding scFv. To accomplish this, we first had to develop a means of radiolabeling small recombinant protein affinity ligands without disrupting their affinity for target antigens (Figure 2A). While full-length antibodies are typically amenable to direct labeling techniques, proteins like scFv are more susceptible to modification of key residues and/or the conditions (eg, oxidation) required for these chemical reactions. Since our prior efforts to directly label αICAM and αPECAM scFv and scFv/TM fusion proteins [14,18] had resulted in loss of binding, we utilized recently reported "sortagged" scFv, which allow site-specific transpeptidation by sortase A (SrtA) and C-terminal addition of fluorophores or functional groups for

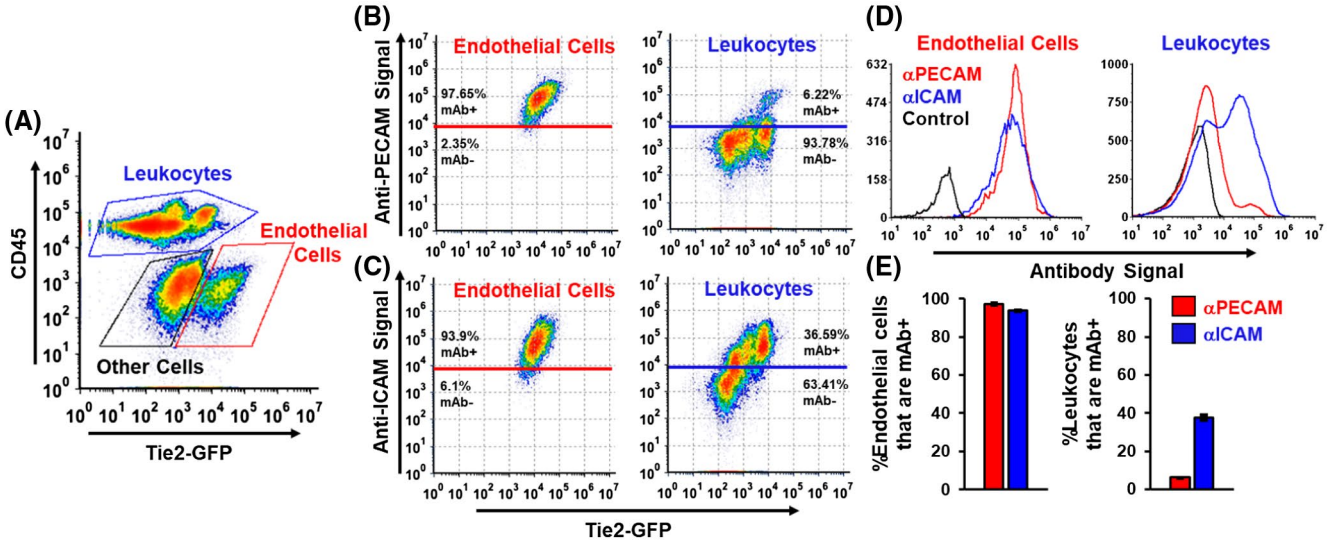

FIGURE 1 Flow cytometric analysis of αICAM and αPECAM antibody distributions among cell types in mouse lungs. A, Density plot for single cell suspension prepared from TIE2-GFP transgenic mouse lungs, after PerCP-aCD45 staining. CD45-high populations are designated as leukocytes and TIE2-GFP-high populations are identified as endothelial cells. B-C, Density plots for cell populations identified as endothelial cells (left panels) or leukocytes (right panels) according to gates established in (A). Data in (B) and (C) correspond to single cell suspensions from TIE2-GFP mice receiving Alexa Fluor 647-aPECAM and Alexa Fluor 647-aICAM fluorescent mAbs, respectively. Horizontal red and blue lines indicate cutoff for positive vs. negative mAb fluorescence, as established by negative-stain control data. D, Histograms for Alexa Fluor 647-aPECAM (red) and Alexa Fluor 647-aICAM (blue) signal in endothelial cells (left panel) and leukocytes (right panel). Black: Control data from TIE2-GFP mice that did not receive mAb. E, Fraction of endothelial cells (left panel) and leukocytes (right panel) positive for Alexa Fluor 647-aPECAM (red, n = 2) or Alexa Fluor 647-aICAM (blue, n = 2)

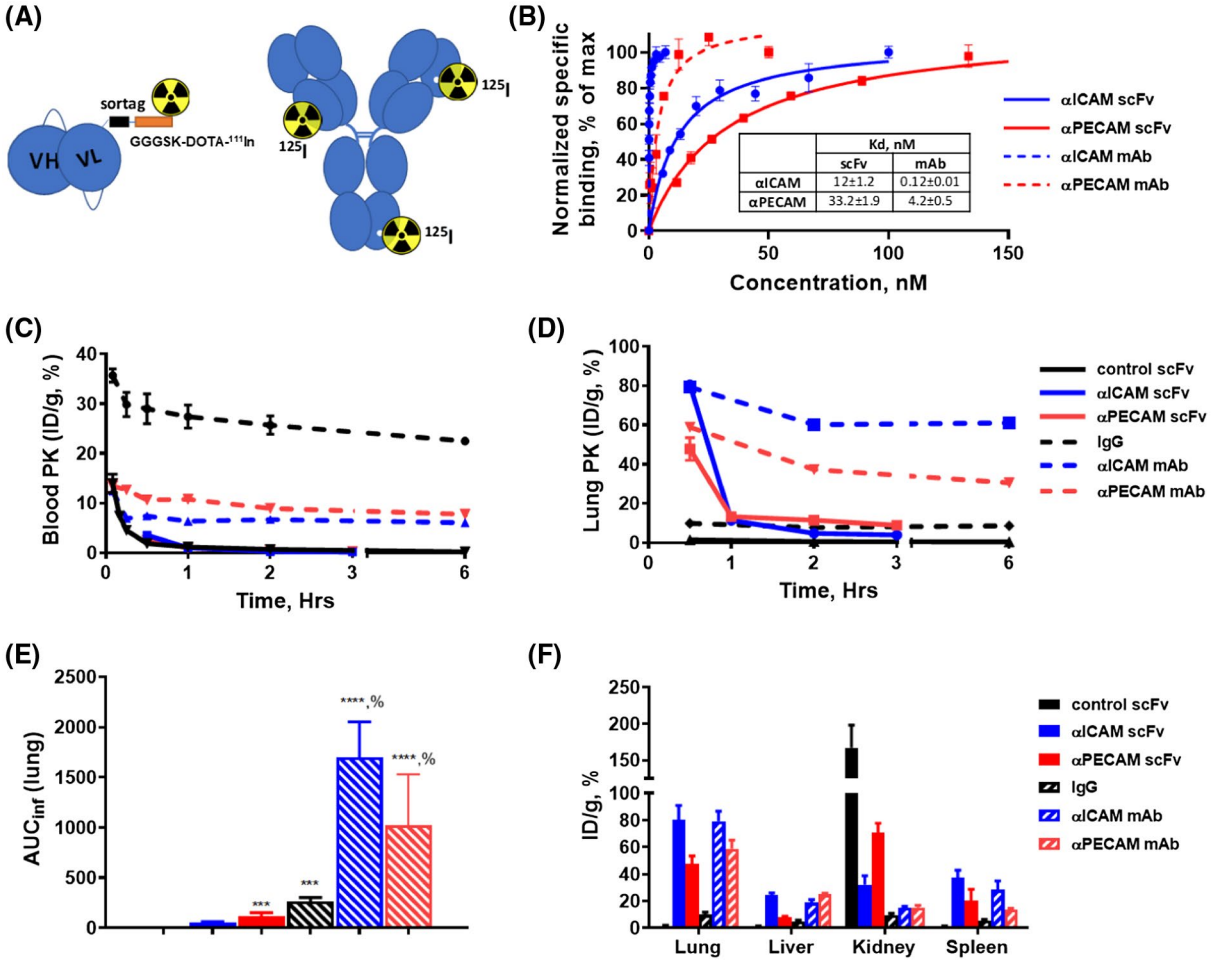

FIGURE 2 Blood and tissue pharmacokinetics of αICAM and αPECAM affinity ligands. A, Schematic showing radiolabeling strategies for scFv vs. mAb. The former were site-specifically labeled with ^{111}In via two-step procedure, whereas the latter were directly radioiodinated. B, Radioimmunoassays of scFv and mAb on ICAM and PECAM-expressing cells vs. control cells. Normalized specific binding was calculated as (total–nonspecific)/maximum. C-F, Blood (C) and lung pharmacokinetics (D) of labeled scFv and mAb, mean ± SD of %ID/g (injected dose per gram of tissue) with n = 4. E, Area under the lung concentration vs. time curve (AUC_{inf}) of targeted and untargeted conjugates, $^{***}P < .001$ and $^{****}P < .0001$, compared to untargeted controls; $\%P < .0001$ mAb compared to scFv. F, 30 min biodistribution data comparing lung uptake with major clearance organs, mean ± SD with n = 4

oriented conjugation to protein cargo.[20] We extended this here to a two-step radiolabeling technique, in which a small peptide incorporating the radiometal chelating group, DOTA (1,4,7,10-tetrazacyclododecane-N,N′,N′′,N′′′-tetraacetic acid) was labeled with ^{111}In and then attached by SrtA to the C-terminal end of the scFv (Figure S2). We compared the affinity of labeled scFv with corresponding parental mAb via RIAs on cells stably expressing ICAM or PECAM vs. control cells. Both αICAM scFv and αPECAM scFv demonstrated saturable, specific binding and nanomolar affinity, with dissociation constants (K_d) of 12 ± 1.2 and 33.2 ± 1.9 nM, respectively. These were approximately 10-fold and 100-fold lower than their parental mAbs (Figure 2B, and Table S1).[14,25]

We injected mice with equimolar doses of radiolabeled αICAM and αPECAM scFv vs. mAb, using non-targeted scFv and nonspecific rat IgG as controls. Both targeted and untargeted scFv cleared from the circulation rapidly ($t_{1/2}$ = 0.984 ± 0.153 hours vs 1.50 ± 0.24 hours vs 1.97 ± 0.21 hours for αICAM, αPECAM, and untargeted, respectively) (Figure 2C, solid lines, Table S1) with high levels of uptake in the kidney, consistent with previous reports indicating efficient renal filtration of scFv (Figure 2F). Full-length antibodies, in contrast, demonstrated prolonged circulation times ($t_{1/2}$ = 21.0 ± 4.6 hours vs 4.3 ± 0.3 hours vs 11.4 ± 2.7 hours for αICAM, αPECAM, and untargeted mAb, respectively). Blood levels of αICAM and αPECAM mAbs demonstrated an initial drop due to target-mediated disposition, but then remained steady, with PK similar to untargeted IgG (Figure 2C, dotted lines).

Despite the significant difference in blood PK, pulmonary biodistribution (a surrogate for endothelial targeting) was

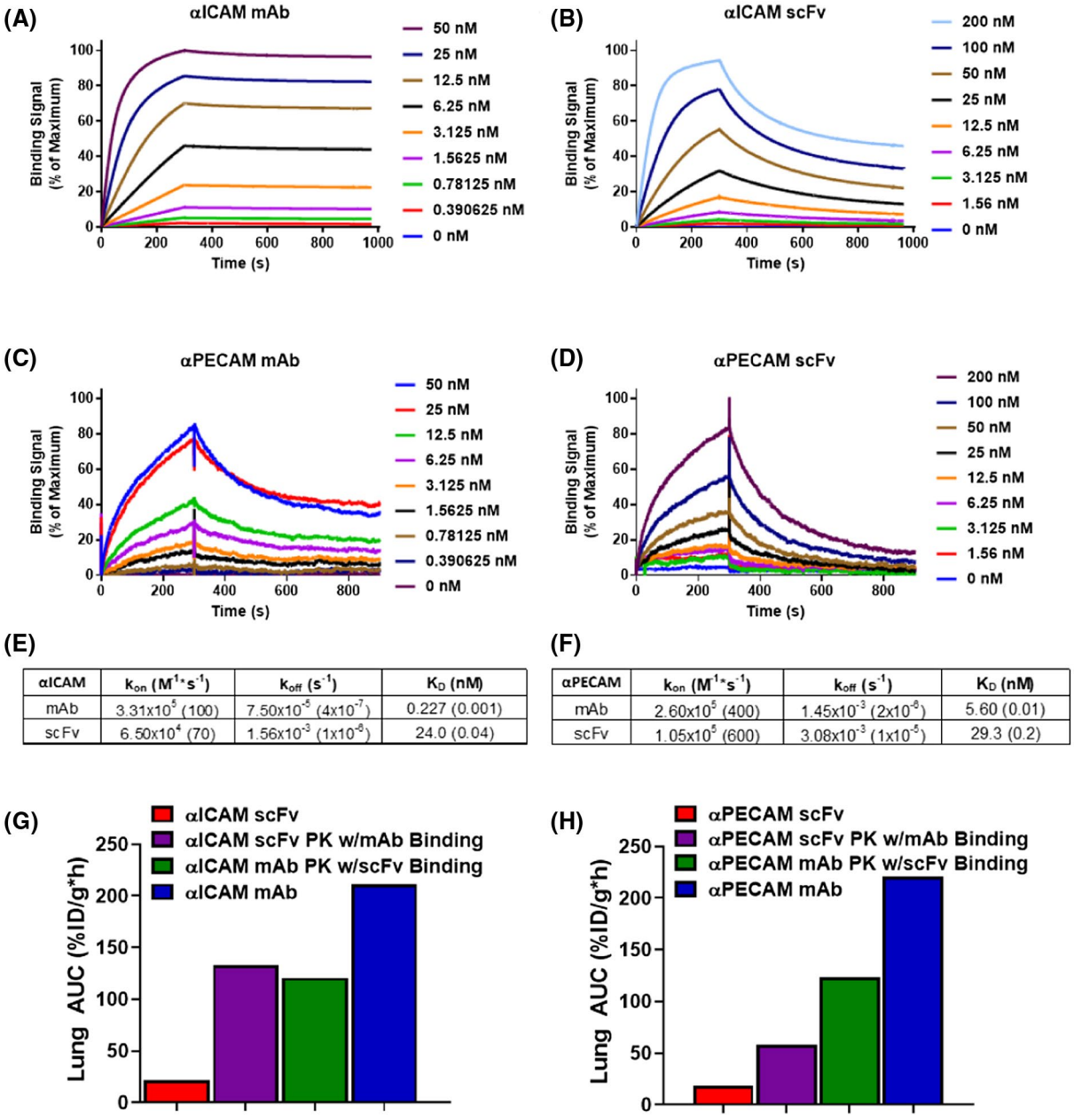

αICAM	k_{on} ($M^{-1}*s^{-1}$)	k_{off} (s^{-1})	K_D (nM)
mAb	$3.31x10^5$ (100)	$7.50x10^{-5}$ ($4x10^{-7}$)	0.227 (0.001)
scFv	$6.50x10^4$ (70)	$1.56x10^{-3}$ ($1x10^{-6}$)	24.0 (0.04)

αPECAM	k_{on} ($M^{-1}*s^{-1}$)	k_{off} (s^{-1})	K_D (nM)
mAb	$2.60x10^5$ (400)	$1.45x10^{-3}$ ($2x10^{-6}$)	5.60 (0.01)
scFv	$1.05x10^5$ (600)	$3.08x10^{-3}$ ($1x10^{-5}$)	29.3 (0.2)

FIGURE 3 Binding kinetics and PBPK modeling simulations of αICAM and αPECAM affinity ligands. A-D, SPR data of monovalent and bivalent affinity ligands – sensorgramsshow multi-cycle kinetics of binding to immobilized ICAM-1 or PECAM-1 under flow. Response units (RUs) are shown as % of maximum binding signal. E-F, Binding parameters for mAb and scFv calculated from SPR assay in a 1:1 global fit. G-H, Experimentally observed vs. predicted lung PK for scFv, mAb, and hypothetical constructs with hybrid characteristics (mAb blood PK with scFv binding characteristics or vice versa) to elucidate the impact of these processes on the kinetics of lung exposure. Changes in model predicted lung AUC_{inf} for αICAM (G) and αPECAM (H) affinity ligands

similar for targeted scFv and mAb at 30 minutes post-injection (Figure 2D) – 80.4% ± 10.6% vs 79.3% ± 4.2% of the injected dose per gram of organ weight (ID/g) for αICAM scFv vs. mAb and 47.7% ± 5.8% vs 58.9% ± 3.6% ID/g for αPECAM scFv vs. mAb. Lung biodistribution was almost entirely antigen specific, as only 1.5% ± 0.5% ID/g of untargeted scFv ($P < .005$ vs. both targeted scFv) and 9.9% ± 0.9% of untargeted mAb ($P < .005$ vs both targeted mAb) were found in the lung at 30 minutes post-intravenous injection. In contrast, marked differences were seen in the lung PK of targeted scFv vs mAb. Lung tissue levels dropped quickly for both αICAM and αPECAM scFv, with 1-hour biodistribution of 11.4% ± 1.7% and 13.4% ± 1.7% ID/g, respectively. Three-hour levels were near baseline (4.0% ± 0.7% for αICAM scFv, 8.9% ± 0.8% for αPECAM scFv and 0.4% ± 0.04% for untargeted control scFv), such that measurement of later time points was not felt to be justified. In contrast, lung levels of targeted mAb declined slowly. At 2 hours post-injection, 60.1% ± 2.1% and 37.3% ± 2.8%

of ID/g of αICAM and αPECAM mAb remained in the lung, while 6-hour levels were 60.9% ± 2.1% and 30.5% ± 0.3% ID/g, respectively. The net result was a marked difference in the area under the curve (AUC_{inf}) of lung concentration vs time (Figure 2E and Table S1) – 1698 ± 352 vs 53.3 ± 7.9 ID/g*hrs for αICAM and 1023 ± 507 vs 114 ± 37 ID/g*hrs for αPECAM ($P < .01$ for both comparisons).

3.3 | αICAM and αPECAM mAb and scFv have similarly low rates of internalization

An important consideration in interpreting radiotracing data is the possibility of internalization of αICAM and αPECAM affinity ligands, which could lead to an overestimation of cell surface targeting. For two decades, the conventional wisdom has been that endocytosis of ICAM-1 and PECAM-1 is quite limited following antibody binding, based on extensive in vitro and in vivo data.[11,26] More recent cell culture studies have refined this understanding, suggesting that endocytosis of PECAM-bound antibodies may depend on their specific epitope,[34] while ICAM-1 may repeatedly internalize bound antibodies and recycle them to the surface.[27,35] In contrast, both ICAM-1 and PECAM-1 are known to rapidly internalize multi-avid species (eg, antibody decorated nanocarriers), which induce clustering and distinct endocytic pathways.[34,36] Given this complexity, we felt it was important to test endocytosis of the specific antibodies used in our radiotracing experiments (clone YN1 for αICAM and clone 390 for αPECAM, respectively) and to compare their rate of internalization with that of monovalent scFv derivatives.[37] Supplemental Figure S3A,B show the results of quantitative radio-internalization assays, which were in line with previous data, indicating fairly limited endocytosis of all surface bound affinity ligands (<20% internalized within 1 hour).

3.4 | Both circulation time and binding characteristics contribute to differences in tissue PK of mAb vs. scFv

We next sought to determine the factors responsible for the marked difference in lung retention time of αICAM and αPECAM mAb vs scFv. While blood PK seemed a likely contributor, we also considered differences in binding parameters and sought to evaluate these using surface plasmon resonance (SPR). As shown in Figure 3A-D, SPR measurements of equilibrium binding affinity for mAb and scFv were similar to those derived from RIAs. SPR, however, also demonstrated differences in binding kinetics, particularly dissociation rate (k_{off}), including a 40-fold difference in αICAM mAb vs scFv (Figure 3E-F). This observation was of particular interest, given the prominent role of k_{off} in determining the length of target engagement.

A semi-physiologically based pharmacokinetic (PBPK) model was constructed (Figure S4), using RIAs, SPR, internalization, and biodistribution data to drive parameter estimates for nonspecific (IgG, untargeted scFv) and target-mediated (αICAM and αPECAM mAb) disposition processes. Since the lung receives the entire cardiac output, lung blood flow was set equal to cardiac output, with the latter derived from widely cited datasets describing physiologic parameters of laboratory mice.[38-40] We sought to minimize the number of fitted parameters, particularly for targeted constructs, in order to improve the predictive capacity of the model. As such, we first fit the model to data for untargeted constructs (Figure S5) to gain an estimate of differences in nonspecific PK processes between constructs. We then fit dose-ranging PK data for mAbs similar to reports available in the literature.[38] Because this approach was able to (1) describe mAb data for both targets (Figure S6), with good confidence in parameters, we then validated the model by applying it to simulate blood and tissue concentration vs. time curves for αICAM and αPECAM scFvs and found that these closely matched experimental data (Figure S7). The fact that the model could predict differences in PK between mAb and scFv strongly supported the notion that the model and its underlying assumptions were relatively reflective of the in vivo situation.

Having established the validity of the model, a variety of simulations were performed to evaluate the relative contributions of blood PK and binding parameters (affinity and kinetics) to the in vivo behavior of the affinity ligands. Specifically, the binding of scFv and mAb were matched with the circulation time of the other entity (ie, scFv binding with mAb circulation time and vice versa) and input into the model to predict lung concentration vs. time AUC. This "crossmatching" of input variables led to predicted AUCs that were intermediate to the experimentally observed values (Figure 3G-H). In the case of αICAM affinity ligands, these parameters appeared roughly equal in importance, whereas for αPECAM, circulation time of mAb seemed to contribute more than binding characteristics. For both antigens, however, the results indicated that a single process could not account for the experimentally observed differences between scFv and mAb, thereby implicating both variables as important contributors to endothelial surface targeting.

3.5 | αICAM and αPECAM mAb and scFv differ markedly in endothelial surface delivery of TM

We next sought to determine the ability of each affinity ligand to deliver thrombomodulin (TM) to the endothelial surface. While past reports have utilized recombinant scFv/TM fusion

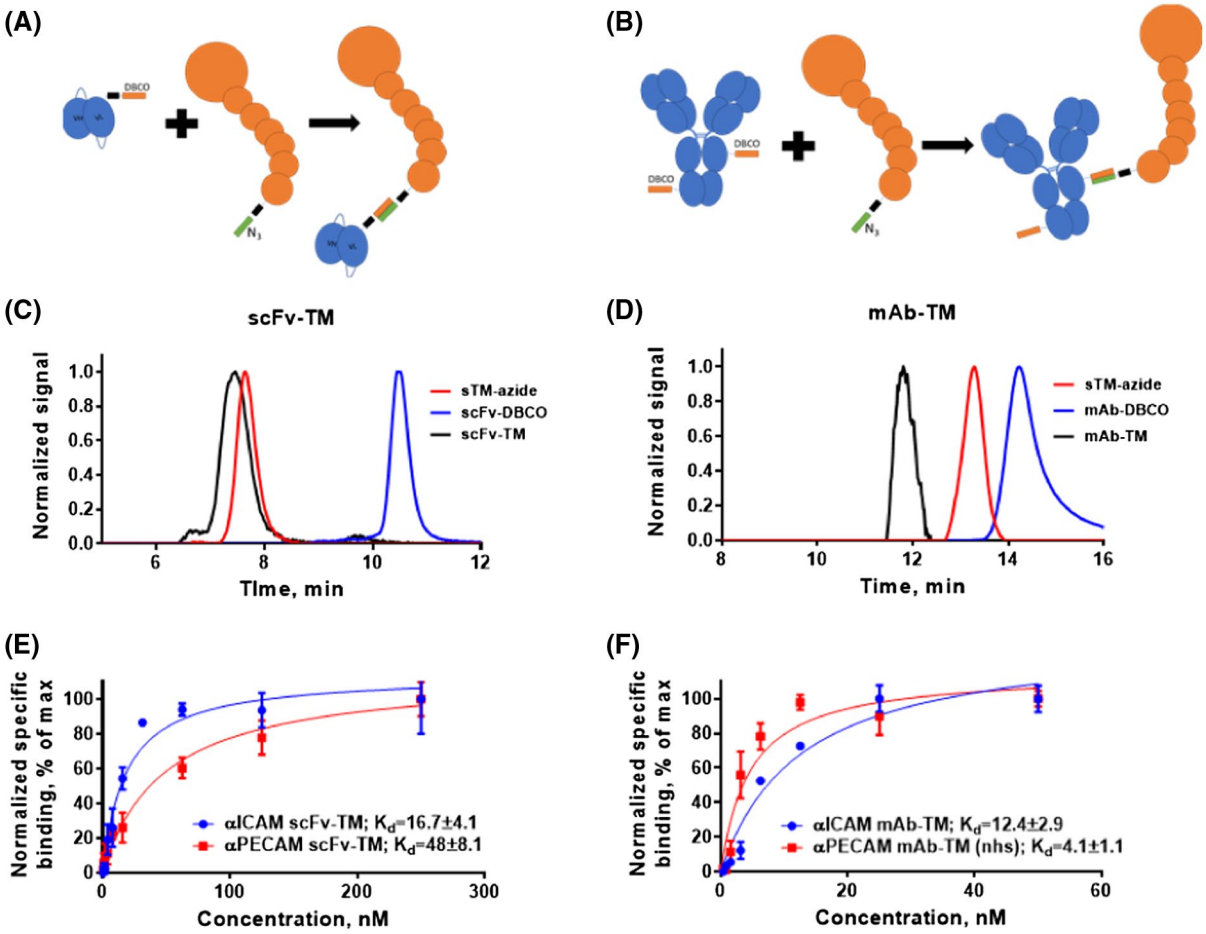

FIGURE 4 Production and characterization of 1:1 scFv- and mAb-TM conjugates. A-B, Schematic showing the combination of site-specific modification and copper-free click chemistry used to produce TM conjugates. In each case, C-terminal azide modified sTM reacts with DBCO-modified affinity ligands, ie scFv (A) or mAb (B). C-D, SEC HPLC traces showing conjugation reaction components and purified 1:1 product. Note: elution times differ because different SEC columns were used. E-F, Radioimmunoassays of scFv-TM (E) and mAb-TM (F) conjugates on ICAM- and PECAM-expressing cells vs. control cells. K_d values are mean ± SD for at least three independent experiments

proteins to achieve this goal, here we produced 1:1 covalent TM conjugates to allow equal comparison of mAb and scFv (Figure 4A,B). Conjugation also allowed for radiolabeling of sTM prior to attachment to affinity ligands, ensuring radiotracing of the cargo protein and preventing any effect of the radiolabeling procedure on affinity ligand binding. Sortase was used to site-specifically modify sTM at its C-terminus (Figure S8A and B), eliminating potential for crosslinking and ensuring equivalent orientation of the cargo protein. All conjugates were evaluated with size exclusion HPLC and 1:1 species were selectively purified (Figure 3C,D and S8C). We also confirmed the function of the cargo protein in each scFv-TM and mAb-TM conjugate, measuring thrombin-dependent activation of protein C (PC) following binding of the conjugates to cells expressing appropriate target antigen. As shown in Figure S8D,E, all conjugates produced dose dependent increase in APC generation.

Before measuring biodistribution, we first determined the equilibrium binding affinity of scFv-TM and mAb-TM conjugates (Figure 4E,F). End-to-end scFv-TM conjugates had largely unaffected affinities (ie, Kd's similar to the isolated affinity ligands). In contrast, the affinities of mAb-TM conjugates, which were heterogeneous in their site of TM attachment to antibody, were less predictable. αPECAM mAb was largely unaffected by TM conjugation (Kd of ~ 4nM for both mAb and mAb-TM), while αICAM mAb was significantly compromised (Kd of 0.12 vs 12 nM for mAb and mAb-TM, respectively, Table S2).

To assess the biodistribution and PK of scFv-TM and mAb-TM conjugates, mice were given a single intravenous injection of ^{125}I-sTM-conjugate, normalizing each dose to fixed amount of sTM cargo (3 μg per mouse). scFv-TM conjugates had limited circulation time (Figure 5A,C), although unlike isolated scFv, the kidney was not the primary organ of clearance (Figure 5D). Surprisingly, neither αICAM nor αPECAM scFv-TM conjugates effectively accumulated in the lung at 30 minutes post-injection (Figure 5B,D), despite affinity for their target antigens.

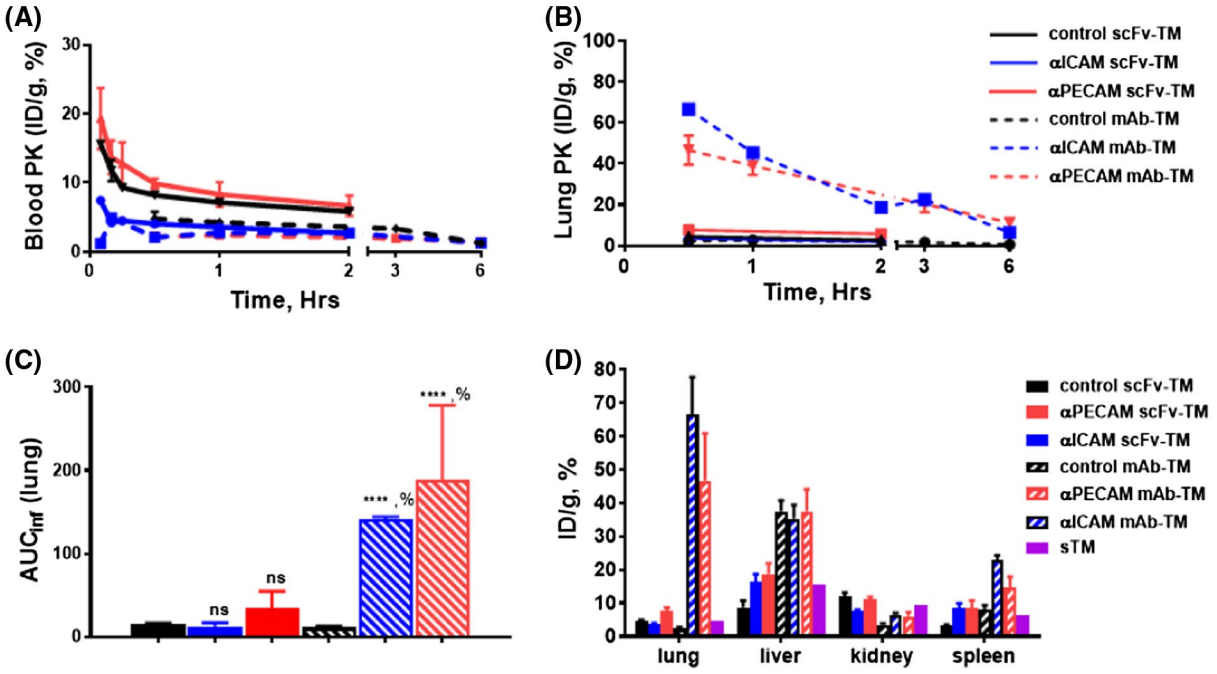

FIGURE 5 Blood and tissue pharmacokinetics of scFv-TM and mAb-TM conjugates. A-D, Blood (A) and lung (B) PK of scFv- and mAb-TM conjugates following single intravenous injection of equimolar dose. Bivalent αICAM and αPECAM mAb-TM, but not scFv-TM, accumulate in the lung and demonstrate prolonged organ residence time, despite having nearly identical blood PK. C, Lung AUC_{inf} of targeted and untargeted conjugates, mean ± SD of %ID/g, with n = 4. ***$P < .001$, ****$P < .0001$, compared to untargeted controls; %$P < .0001$, mAb-TM compared to scFv-TM. D, 30 min biodistribution showing uptake in lung vs. clearance organs, mean ± SD, with n = 4. Unlike isolated scFv, the kidney is not the primary organ of clearance for scFv-TM conjugates

Radiotracing of mAb-TM conjugates also produced unexpected results. Similar to scFv-TM conjugates, but in stark contrast to isolated mAbs, mAb-TM conjugates had limited circulation time (Figure 5A,C). This applied even to untargeted IgG-TM, indicating that target-mediated disposition was not the primary factor. The liver and spleen were the dominant clearance organs for both targeted and untargeted scFv-TM and mAb-TM, which closely matched the distribution of sTM alone (Figure 5D).

Unlike their scFv-TM counterparts, however, mAb-TM conjugates both accumulated in the lung–66.6% ± 11.1% for αICAM and 46.7% ± 14.2% for αPECAM (vs 2.7% ± 0.5% ID/g for IgG, $P < .005$)–and were retained for several hours. Lung AUCs for mAb-TM conjugates were roughly an order of magnitude lower than free antibodies, but far superior to scFv-TM conjugates (AUC_{inf} 141 ± 3.2 vs 12.4 ± 4.2 ID/g*hrs for αICAM and 188 ± 90 vs 34.7 ± 19.9 ID/g*hrs for αPECAM mAb vs scFv, $P < .005$) (Figure 5C, and Table S3).

The semi-PBPK model was fit to obtain estimates of non-specific disposition parameters for untargeted IgG-sTM and scFv-sTM conjugates (Figure S9). Simulations of blood and lung PK for mAb-sTM conjugates provided reasonable characterization of observed data (Figure S10), while simulations with scFv-sTM conjugates grossly overpredicted lung uptake (Figure S11).

3.6 | End-to-end conjugation of αICAM mAb to TM further improves lung targeting and residence time

The superiority of mAb-TM vs. scFv-TM conjugates, in spite of seemingly equivalent blood PK, further underscored the importance of bivalent target engagement in determining the in vivo behavior of endothelial surface targeted protein therapeutics. We hypothesized that oriented, end-to-end conjugation of TM to αICAM mAb might further improve surface targeting, given the impact of TM conjugation on the binding affinity of the NHS ester-modified antibody. To accomplish this, we took advantage of a recently reported modified αICAM antibody, mAb-ss, which was engineered by CRISPR modification of the parental YN1 hybridoma to insert a sortag and triple FLAG tag at the C-terminus of each heavy chain.[23] Sortase-modification of mAb-ss with DBCO-containing peptide and subsequent reaction with ^{125}I-labeled, site-specifically modified sTM-azide resulted in C-terminus to C-terminus conjugation (Figure 6A). As with previous conjugates, reaction mixtures were characterized by SEC HPLC, which was used to selectively purify 1:1 species (Figure 6B).

Figure 6C,D compare the blood and lung biodistribution of αICAM mAb-ss-TM vs. non-oriented mAb-TM following intravenous injection of a single, equimolar dose. No

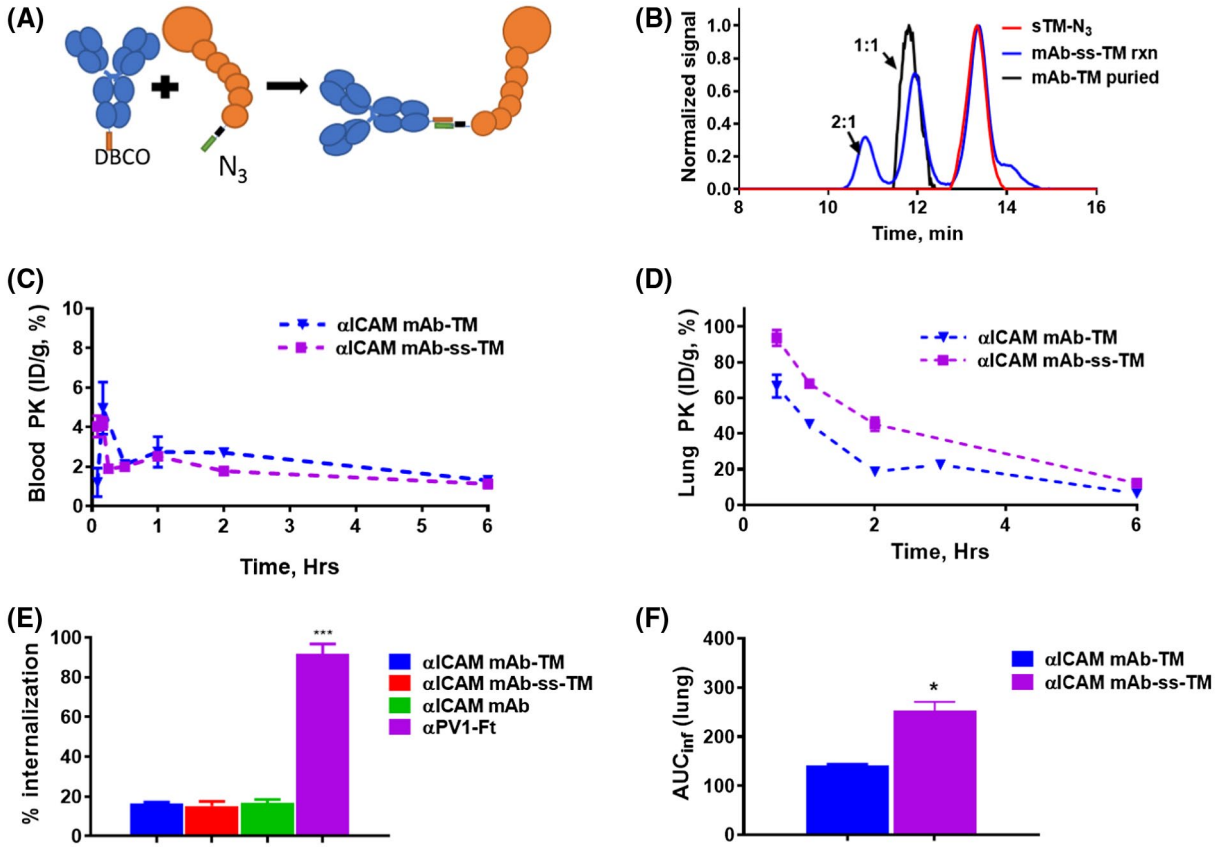

FIGURE 6 End-to-end conjugation of αICAM mAb to TM further enhances delivery to vascular endothelium. A, Schematic showing DBCO modification of αICAM mAb-ss, which contains a C-terminal sortag, and 'end-to-end' conjugation to sTM-azide, preserving bivalent binding of the affinity ligand. B, SEC HPLC traces of unpurified mAb-ss-TM reaction mixture (blue) showing 1:1 and 1:2 products, as well as the final purified 1:1 mAb-ss-TM conjugate (black line). C and D, Blood and lung PK of αICAM mAb-ss-TM vs. non-oriented mAb-TM following intravenous injection of a single, equimolar dose. E, Internalization assay of αICAM mAb-ss-TM vs. non-oriented mAb-TM conjugates vs. mAb alone on endothelial cells (bEnd3). Anti-PV1-Ft conjugate was used as a positive control. ***$P < .001$. F) Lung AUCinf of αICAM mAb-ss-TM is significantly greater than non-oriented αICAM mAb-TM (*$P < .05$)

difference was seen in blood PK, but end-to-end conjugates demonstrated superior lung biodistribution at 30 minutes post-injection (93.6 ± 8.9 vs 66.6% ± 11.1%ID/g, $P < .05$), as well as a nearly two-fold improvement in lung AUC_{inf} (253 ± 18 ID/g*hrs for αICAM mAb-ss-TM vs. 141 ± 3.2 ID/g*hrs for non-oriented mAb-TM, $P < .05$, Figure 6F). We again tested internalization to ensure that radiotracing reflected surface targeting, this time using mAb-ss-TM and a fluorescence-based assay on mouse endothelial cells. As shown in Figure 5F, mAb-ss-TM conjugates showed similar, low levels of internalization to free αICAM mAb and non-oriented αICAM mAb-TM conjugates. A highly internalized, PVLAP-targeted conjugate was used as a positive control (Figure 6E).

4 | DISCUSSION

At first glance, endothelial surface delivery appears to be one of the simplest of all targeted pharmacologic strategies. ECs form not only the largest cellular surface area in the human body, but also a readily accessible membrane decorated with surface molecules evolved to interact with circulating blood components.[36] Like other seemingly straightforward drug delivery applications (eg, anti-neoplastic ADCs),[39,40] however, execution has proven more challenging than initially expected. Some EC surface targets, like the receptors for transferrin and insulin, are poorly suited for surface anchoring, as their biologic functions necessitate rapid internalization in response to binding.[41] Others, like the cell adhesion molecules, are appropriate for mono- or bivalent affinity ligands, but initiate endocytic pathways upon engagement by multi-avid nanoparticles and large, cross-linked protein conjugates.[41] Beyond these biological hurdles, relatively little is known about the optimal characteristics of affinity ligands meant for sustained surface localization, or how these properties (eg, binding affinity, circulation time) may be affected by attachment of protein cargo.[42] While long-circulating antibodies given at a saturating dose have been used to induce prolonged blockade of endothelial surface targets

like ICAM-1 and P-selectin,[43-45] the best means of achieving sustained surface display of protein cargo remains unknown.

These issues are of particular interest given substantial preclinical data suggesting the utility of anchoring biotherapeutics to endothelial surfaces.[11,14,18,19,36,46,47] Preliminary studies have mostly used monovalent scFv fusion proteins, favored based on their minimal rate of internalization and uniform molecular conformation. Examples of cargo successfully delivered via scFv fusion protein include single-chain urokinase-type plasminogen activator (scuPA), the first recombinant protein to be fused to anti-PECAM scFv.[48] Intravenous injection of this therapeutic was shown to prevent occlusive thrombosis in both lung and brain vasculature, albeit only when administered immediately prior to thrombotic challenge.[48] Neither the PK nor the therapeutic window were fully evaluated and the approach has been largely supplanted by efforts to target erythrocytes and platelets as circulating carriers for fibrinolytics.[49,50] Interestingly, endogenously produced tissue plasminogen activator (tPA) has since been shown to assemble on the luminal membrane following secretion by ECs and this localization seems to be important in generating effective clot lysis.[51] It remains an intriguing and unaddressed question if targeting recombinant tPA to the local endothelial surface is possible in the presence of occlusive clot and if this strategy could be a viable alternative to local (ie, catheter-mediated) delivery of tPA.

The best studied cargo for endothelial surface delivery, however, is thrombomodulin, the key membrane-bound component of the protein C pathway. Together with its surface partner, EPCR, TM accelerates thrombin-dependent activation of protein C and contributes to nearly all homeostatic functions of the vascular endothelium. Indeed, its disappearance from the luminal membrane in the presence of stasis, inflammation, and oxidative stress seems to be a bellwether of change from healthy endothelium to the leaky, pro adhesive, and prothrombotic phenotype characteristic of diseased tissue. Delivery of recombinant sTM to the endothelial surface has been accomplished via scFv to both PECAM and ICAM,[14,17,18,52] although the subcellular localization of the latter has been found to produce superior partnering with EPCR and enhanced functional activity. The ability of CAM-anchored TM to reverse endothelial dysfunction has been tested in a variety of settings–most recently in a human whole blood microfluidic model, where it was found to restore the antithrombotic phenotype of cytokine-activated endothelial monolayers.[19]

The current manuscript not only provides answers regarding the optimal means of endothelial surface delivery of TM, but also some insights into factors which contribute to targeting and sustained surface localization. First of all, our biodistribution data indicate that both mono- and bivalent affinity ligands are capable of robust targeting to PECAM-1 and ICAM-1. While not entirely surprising given the availability and accessibility of these highly expressed surface antigens, the near equivalence of mAb and scFv lung concentration at 30 minutes post-injection–despite at least an order of magnitude difference in their K_d–suggests that equilibrium binding affinity may not be a critical factor in determining biodistribution at early time points (or at least that its impact is limited beyond a certain point). In contrast, the marked difference in scFv vs mAb lung concentration over time (as quantified by the AUC) indicates key differences in the ability of these affinity ligands to maintain surface localization. Given the rapid renal filtration of scFv and prolonged FcRn-driven circulation of full-length antibodies, it is tempting to attribute these findings entirely to differences in blood PK. In this line of thinking, both classes of affinity ligand would readily bind their endothelial targets after injection, but the blood concentration of scFv would rapidly drop below levels needed to sustain target engagement, whereas mAb would reach a stable equilibrium between bound and circulating forms.

While plausible, this simplified analysis fails to incorporate the full range of properties of affinity ligand and target (eg, binding affinity, kinetics, expression, and internalization), or the multitude of physiologic processes (eg, blood flow rates, organ volumes) relevant to biodistribution. Indeed, relatively few efforts have been made to develop mechanistic understanding of the PK of endothelial surface targeting, despite significant work done on modeling intracellular delivery [53-55] and transcytosis.[56] To our knowledge, the only example of a mechanistic model of cell surface anchoring has been in the case of bispecific T-cell engagers,[57,58] making the PBPK approach described here relatively unique. The potential value of the current model is demonstrated by a series of simulations, in which various characteristics of mAb and scFv are "swapped" to determine their relative contribution to lung biodistribution and PK. The results paint a more nuanced picture of the in vivo behavior of these affinity ligands, in which both circulation time and bivalent target engagement, with its associated prolongation of dissociation kinetics, contribute to surface retention. In addition to helping explain existing data, the model suggests future experimental directions, including construction of hybrid affinity ligands (eg, bivalent scFv with no Fc fragment or, conversely, an scFv-Fc fusion protein with just one binding arm) and affinity maturation with selection for slow dissociation rates.

Biodistribution data from TM conjugates provide some confirmation of accuracy and value of our PBPK model. In particular, the fact that single injections of both PECAM-1 and ICAM-1 targeted mAb-TM provide several hours of lung endothelial surface targeting and that their AUCs remain superior to those of corresponding scFv-TM, despite blood PK being indistinguishable, supports the

model-derived conclusion that bivalent target engagement is a key contributor to prolonged surface localization. This notion is further bolstered by the enhanced lung PK of αICAM mAb-ss-TM, which differs only in its site-specific attachment of the cargo at the site least likely to interfere with bivalent binding. In spite of the predictions of our model, we cannot completely exclude the possibility that the Fc fragment, and not bivalent binding, is responsible for some of the differences in in vivo behavior of mAb-TM vs. scFv-TM conjugates. mAb-TM may interact with a variety of non-endothelial cell types via Fc receptors,[59] a feature not included in our model. Likewise, FcRn interaction could play a role,[60] as it clearly does in the behavior of isolated affinity ligands, although the similarity of the blood PK of mAb-TM and scFv-TM would argue against this. As mentioned above, definitive conclusions will require additional experimentation–for example, the synthesis and testing of $F(ab')_2$-TM conjugates.

It is also worth noting that the existing PBPK model is not without limitations. Binding parameters derived from in vitro experiments (SPR, RIAs) may not reflect the kinetics which occur in vivo. Likewise, our model does not account for differences in expression or localization of cell adhesion molecules in the endothelium of different organs or in disease states. Similarly, our existing data and modeling only apply to healthy mice and, given the desired applications, it will be an important next step to characterize the blood and tissue PK of endothelial-surface targeted therapeutics in relevant animal models of human disease. Beyond organ distribution, the uptake of PECAM-1 and particularly ICAM-1 targeted therapeutics by non-endothelial cell types will also need to be carefully examined in disease states. In addition, our existing model will need to be modified to account for the apparent lack of endothelial targeting of scFv-TM conjugates. While the precise reasons remain unclear, the most likely explanation is that conjugates with monovalent affinity ligands, despite having preserved equilibrium binding affinity in vitro, engage their surface targets so briefly and are cleared so quickly in vivo that lung biodistribution cannot be distinguished from background. This raises the interesting question of why the TM conjugates (and sTM alone) are cleared so rapidly. The pattern of clearance suggests active uptake into the liver and likely excretion through bile into the intestine. The data are in agreement with a previous study that reported rapid clearance of ^{125}I-labeled mouse lung thrombomodulin,[47] although they contradict studies of ART123, recombinant human sTM made in Chinese hamster ovary cells, which has been reported to circulate for several hours in rat, monkey, and human, and which appears to be excreted mainly via the kidneys in healthy human volunteers.[61] Whether these inconsistencies are a result of variability in species or related to differences in recombinant protein production in mammalian vs. insect cells is unknown.

In summary, we report the first systematic evaluation of the blood and tissue PK of monovalent vs. bivalent endothelial affinity ligands and the first exploration of factors determining surface localization of an endothelial-targeted protein therapeutic in vivo. Our results clearly favor oriented attachment of recombinant mouse sTM to bivalent affinity ligands and provide critical information regarding dosing for future evaluation of pharmacodynamics and efficacy in lung injury models. Of more general significance, they provide a starting point and blueprint for studies aimed at improving PBPK modeling of endothelial cell surface targeting.

5 | PHARMACOKINETIC MODELING SECTION

5.1 | Supplemental methods

5.1.1 | Model structure

A semi-physiologically based pharmacokinetic (sPBPK) model was developed to describe the in vivo behavior of mAbs, scFvs, and conjugates with thrombomodulin (Figure S1). In the model, the central volume of distribution was linked to a physiologically structured lung compartment. The model was parameterized using physiologically relevant values for blood flow (Q_{organ}) and organ volume (V_{organ}), as described by Shah and Betts.[62] Lung was further sub-divided into volumes representing the vascular space, endosomal space of the vascular endothelium, and interstitial space (Figure S4).

Drug was assumed to enter the lung from the central compartment into the lung vascular space. From the vascular space, drug was assumed to be able to either: (1) leave the tissue and return to the central compartment by the blood flow rate, (2) directly move into the interstitial space via the transendothelial flux rate (representative of diffusion and convection), or (3) bind to target molecules accessible from the vasculature.

Direct movement of drug into the interstitial space was described by a single term (*TER*) representative of both convection and diffusion and assumed to be directly proportional to organ blood flow. Drug within the interstitial space was assumed to leave the tissue via lymphatic drainage (L_{organ}) at a rate directly proportional to tissue blood flow. Following drainage into the lymphatics, it was assumed that drug would return to the venous circulation at a rate consistent with the tissue lymph flow.

Binding of antibody to target receptor was assumed to occur via second-order association (k_{on}) and first-order

dissociation (k_{off}) rate constants, with the equilibrium affinity (K_D) being determined as the ratio of k_{off}/k_{on}. Binding kinetic parameters were fixed to values obtained using surface plasmon resonance (SPR). Target expression (R_{tot}) was calculated for the central and lung spaces (see Parameter Estimation) and basal target turnover was described by first-order degradation (k_{deg}) and zero-order synthesis (k_{syn}) rate constants, with $R_{tot} = k_{syn}/k_{deg}$. The internalization rate of antibody-target complexes was estimated to be at a similar rate as free target, based on model fitted values.

5.1.2 | Parameter estimation

Parameter relating to nonspecific (eg, nontarget-mediated) disposition were obtained by fitting the model to blood and lung concentration vs. time data obtained for pooled rat IgG, untargeted scFv (R6.5), and conjugates. Parameters related to target expression, target turnover, and mAb-target complex internalization were obtained by fitting the model to dose-escalation blood and lung concentration vs. time data for ICAM- (YN1) and PECAM-targeted (390) mAbs.

5.1.3 | Model predictions

The blood and tissue pharmacokinetics of targeted scFvs and mAb conjugates were predicted by performing simulations, with no additional fitting of parameters, using the estimated parameters for untargeted molecules and those for target expression and interactions.

5.1.4 | Model evaluation

Simulations were performed using the final parameter estimates in order to predict vascular concentrations (sum of free and endothelial bound) of targeting ligand in the lung. These values were then compared to in vitro dose-response curves for Activated Protein C (APC) generation to make predictions regarding potentially efficacious doses of conjugates with soluble thrombomodulin (sTM).

CONFLICT OF INTEREST

Authors declare no conflict of interest.

AUTHOR CONTRIBUTIONS

R. Yu. Kiseleva, V. R. Muzykantov, and C. F. Greineder designed research; R. Yu. Kiseleva, P. G. Glassman, K. M. LeForte, L. R. Walsh, C. H. Villa, V. V. Shuvaev, O. A. Marcos-Contreras, J. W. Myerson, P. A. Aprelev, and C. F. Greineder performed research and analyzed data; R. Yu. Kiseleva, P. G. Glassman, and C. F. Greineder wrote the paper.

REFERENCES

1. Aird WC. Endothelial cell heterogeneity. *Cold Spring Harb Perspect Med*. 2012;2(1):a006429.
2. Lamberti G, Kiani MF, Wang B. Improving the binding efficiency of a vascular drug delivery system by using a dual-receptor targeting strategy. In *2012 38th Annual Northeast Bioengineering Conference (NEBEC)*. Philadelphia, PA; 2012.
3. Shuvaev VV, Christofidou-Solomidou M, Scherpereel A, et al. Factors modulating the delivery and effect of enzymatic cargo conjugated with antibodies targeted to the pulmonary endothelium. *J Control Release*. 2007;118(2):235-244.
4. Danilov SM, Muzykantov VR, Martynov AV, et al. Lung is the target organ for a monoclonal antibody to angiotensin-converting enzyme. *Lab Invest*. 1991;64(1):118-124.
5. Jacobson BS, Schnitzer JE, McCaffery M, Palade GE. Isolation and partial characterization of the luminal plasmalemma of microvascular endothelium from rat lungs. *Eur J Cell Biol*. 1992;58(2):296-306.
6. Myerson JW, Braender B, Mcpherson O, et al. Flexible nanoparticles reach sterically obscured endothelial targets inaccessible to rigid nanoparticles. *Adv Mater*. 2018;30(32):e1802373.
7. Shuvaev VV, Kiseleva RY, Arguiri E, et al. Targeting superoxide dismutase to endothelial caveolae profoundly alleviates inflammation caused by endotoxin. *J Controlled Release*. 2018;272:1-8.
8. Muro S, Muzykantov VR. Targeting of antioxidant and anti-thrombotic drugs to endothelial cell adhesion molecules. *Curr Pharm Des*. 2005;11(18):2383-2401.
9. Newman PJ. The role of PECAM-1 in vascular cell biology. *Ann NY Acad Sci*. 1994;714:165-174.
10. Lertkiatmongkol P, Liao D, Mei H, et al. Endothelial functions of platelet/endothelial cell adhesion molecule-1 (CD31). *Curr Opin Hematol*. 2016;23(3):253-259.
11. Murciano J-C, Muro S, Koniaris L, et al. ICAM-directed vascular immunotargeting of antithrombotic agents to the endothelial luminal surface. *Blood*. 2003;101(10):3977-3984.
12. Muro S, Schuchman EH, Muzykantov VR. Lysosomal enzyme delivery by ICAM-1-targeted nanocarriers bypassing glycosylation- and clathrin-dependent endocytosis. *Mol Ther*. 2006;13(1):135-141.
13. Chittasupho C, Xie S-X, Baoum A, et al. ICAM-1 targeting of doxorubicin-loaded PLGA nanoparticles to lung epithelial cells. *Eur J Pharm Sci*. 2009;37(2):141-150.
14. Greineder CF, Chacko A-M, Zaytsev S, et al. Vascular immunotargeting to endothelial determinant ICAM-1 enables optimal partnering of recombinant scFv-thrombomodulin fusion with endogenous cofactor. *PLoS One*. 2013;8(11):e80110.
15. Greineder CF, Howard MD, Carnemolla R, et al. Advanced drug delivery systems for antithrombotic agents. *Blood*. 2013;122(9):1565-1575.
16. Kiseleva RY, Glassman PM, Greineder CF, Hood ED, Shuvaev VV, Muzykantov VR Targeting therapeutics to endothelium: are we there yet? *Drug Deliv Transl Res*. 2017;8(4):883-902.
17. Greineder CF, Brenza JB, Carnemolla R, et al. Dual targeting of therapeutics to endothelial cells: collaborative enhancement of delivery and effect. *FASEB J*. 2015;29(8):3483-3492.

18. Ding B-S, Hong N, Christofidou-Solomidou M, et al. Anchoring fusion thrombomodulin to the endothelial lumen protects against injury-induced lung thrombosis and inflammation. *Am J Respir Crit Care Med*. 2009;180(3):247-256.
19. Greineder CF, Johnston IH, Villa CH, et al. ICAM-1-targeted thrombomodulin mitigates tissue factor-driven inflammatory thrombosis in a human endothelialized microfluidic model. *Blood Adv*. 2017;1(18):1452-1465.
20. Greineder CF, Villa CH, Walsh LR, et al. Site-specific modification of single-chain antibody fragments for bioconjugation and vascular immunotargeting. *Bioconjug Chem*. 2018;29(1):56-66.
21. Scherpereel A, Rome JJ, Wiewrodt R, et al. Platelet-endothelial cell adhesion molecule-1-directed immunotargeting to cardiopulmonary vasculature. *J Pharmacol Exp Ther*. 2002;300(3):777-786.
22. Kiseleva RY, Greineder CF, Villa CH, et al. Vascular endothelial effects of collaborative binding to platelet/endothelial cell adhesion molecule-1 (PECAM-1). *Sci Rep*. 2018;8(1):1510.
23. Khoshnejad M, Brenner JS, Motley W, et al. Molecular engineering of antibodies for site-specific covalent conjugation using CRISPR/Cas9. *Sci Rep*. 2018;8(1):1760.
24. Coll Ferrer MC, Shuvaev VV, Zern BJ, et al. Icam-1 targeted nanogels loaded with dexamethasone alleviate pulmonary inflammation. *PLoS One*. 2014;9(7):e102329.
25. Kiseleva R, Greineder CF, Villa CH, et al. Mechanism of collaborative enhancement of binding of paired antibodies to distinct epitopes of platelet endothelial cell adhesion molecule-1. *PLoS One*. 2017;12(1):e0169537.
26. Muzykantov VR, Christofidou-Solomidou M, Balyasnikova I, et al. Streptavidin facilitates internalization and pulmonary targeting of an anti-endothelial cell antibody (platelet-endothelial cell adhesion molecule 1): a strategy for vascular immunotargeting of drugs. *Proc Natl Acad Sci*. 1999;96(5):2379-2384.
27. Ghaffarian R, Muro S. Distinct subcellular trafficking resulting from monomeric vs multimeric targeting to endothelial ICAM-1: implications for drug delivery. *Mol Pharm*. 2014;11(12):4350-4362.
28. Brenner JS, Bhamidipati K, Glassman PM, et al. Mechanisms that determine nanocarrier targeting to healthy versus inflamed lung regions. *Nanomedicine*. 2017;13(4):1495-1506.
29. Roki N, Tsinas Z, Solomon M, et al. Unprecedently high targeting specificity toward lung ICAM-1 using 3DNA nanocarriers. *J Control Release*. 2019;305:41-49.
30. Marcos-Contreras OA, Brenner JS, Kiseleva RY, et al. Combining vascular targeting and the local first pass provides 100-fold higher uptake of ICAM-1-targeted vs untargeted nanocarriers in the inflamed brain. *J Control Release*. 2019;301:54-61.
31. Muro S, Gajewski C, Koval M, et al. ICAM-1 recycling in endothelial cells: a novel pathway for sustained intracellular delivery and prolonged effects of drugs. *Blood*. 2005;105(2):650-658.
32. Brenner JS, Kiseleva RY, Glassman PM, et al. EXPRESS: the new frontiers of the targeted interventions in the pulmonary vasculature: precision and safety. *Pulm Circ*. 2017;8(1):2045893217752329.
33. Parhiz H, Shuvaev VV, Pardi N, et al. PECAM-1 directed re-targeting of exogenous mRNA providing two orders of magnitude enhancement of vascular delivery and expression in lungs independent of apolipoprotein E-mediated uptake. *J Control Release*. 2018;291:106-115.
34. Muro S, Wiewrodt R, Thomas A, et al. A novel endocytic pathway induced by clustering endothelial ICAM-1 or PECAM-1. *J Cell Sci*. 2003;116(Pt 8):1599-1609.
35. Ghaffarian R, Roki N, Abouzeid A, et al. Intra- and trans-cellular delivery of enzymes by direct conjugation with non-multivalent anti-ICAM molecules. *J Control Release*. 2016;238:221-230.
36. Shuvaev VV, Brenner JS, Muzykantov VR. Targeted endothelial nanomedicine for common acute pathological conditions. *J Control Release*. 2015;219:576-595.
37. Shuvaev VV, Muro S, Arguiri E, et al. Size and targeting to PECAM vs ICAM control endothelial delivery, internalization and protective effect of multimolecular SOD conjugates. *J Control Release*. 2016;234:115-123.
38. Shah DK, Balthasar JP. Predicting the effects of 8C2, a monoclonal anti-topotecan antibody, on plasma and tissue disposition of topotecan. *J Pharmacokinet Pharmacodyn*. 2014;41(1):55-69.
39. Allen TM. Ligand-targeted therapeutics in anticancer therapy. *Nat Rev Cancer*. 2002;2(10):750-763.
40. Drachman JG, Senter PD. Antibody-drug conjugates: the chemistry behind empowering antibodies to fight cancer. *Hematology Am Soc Hematol Educ Program*. 2013;2013:306-310.
41. Muzykantov VR. Targeted drug delivery to endothelial adhesion molecules. *ISRN Vasc Med*. 2013;2013:1-27.
42. Agarwal P, Bertozzi CR. Site-specific antibody-drug conjugates: the nexus of bioorthogonal chemistry, protein engineering, and drug development. *Bioconjug Chem*. 2015;26(2):176-192.
43. Wagner N-M, Bierhansl L, Nöldge-Schomburg G, et al. Toll-like receptor 2-blocking antibodies promote angiogenesis and induce ERK1/2 and AKT signaling via CXCR4 in endothelial cells. *Arterioscler Thromb Vasc Biol*. 2013;33(8):1943-1951.
44. Schneider D, Berrouschot J, Brandt T, et al. Safety, pharmacokinetics and biological activity of enlimomab (anti-ICAM-1 antibody): an open-label, dose escalation study in patients hospitalized for acute stroke. *Eur Neurol*. 1998;40(2):78-83.
45. Schmitt C, Abt M, Ciorciaro C, et al. First-in-man study with inclacumab, a human monoclonal antibody against P-selectin. *J Cardiovasc Pharmacol*. 2015;65(6):611-619.
46. Christofidou-Solomidou M, Scherpereel A, Wiewrodt R, et al. PECAM-directed delivery of catalase to endothelium protects against pulmonary vascular oxidative stress. *Am J Physiol Lung Cell Mol Physiol*. 2003;285(2):L283-L292.
47. Shuvaev VV, Han J, Yu KJ, et al. PECAM-targeted delivery of SOD inhibits endothelial inflammatory response. *FASEB J*. 2011;25(1):348-357.
48. Ding B-S, Gottstein C, Grunow A, et al. Endothelial targeting of a recombinant construct fusing a PECAM-1 single-chain variable antibody fragment (scFv) with prourokinase facilitates prophylactic thrombolysis in the pulmonary vasculature. *Blood*. 2005;106(13):4191-4198.
49. Fuentes RE, Zaitsev S, Ahn HS, et al. A chimeric platelet-targeted urokinase prodrug selectively blocks new thrombus formation. *J Clin Invest*. 2016;126(2):483-494.
50. Villa CH, Anselmo AC, Mitragotri S, et al. Red blood cells: supercarriers for drugs, biologicals, and nanoparticles and inspiration for advanced delivery systems. *Adv Drug Deliv Rev*. 2016;106(Pt A):88-103.
51. Murciano J-C, Medinilla S, Eslin D, et al. Prophylactic fibrinolysis through selective dissolution of nascent clots by tPA-carrying erythrocytes. *Nat Biotechnol*. 2003;21(8):891-896.

52. Zaitsev S, Kowalska MA, Neyman M, et al. Targeting recombinant thrombomodulin fusion protein to red blood cells provides multifaceted thromboprophylaxis. *Blood*. 2012;119(20):4779-4785.
53. Cilliers C, Guo H, Liao J, et al. Multiscale modeling of antibody-drug conjugates: connecting tissue and cellular distribution to whole animal pharmacokinetics and potential implications for efficacy. *AAPS J*. 2016;18(5):1117-1130.
54. Wang-Lin SX, Zhou C, Kamath AV, et al. Minimal physiologically-based pharmacokinetic modeling of DSTA4637A, A novel THIOMAB antibody antibiotic conjugate against *Staphylococcus aureus*, in a mouse model. *MAbs*. 2018;10(7):1131-1143.
55. Khot A, Tibbitts J, Rock D, et al. Development of a translational physiologically based pharmacokinetic model for antibody-drug conjugates: a case study with T-DM1. *AAPS J*. 2017;19(6):1715-1734.
56. Gadkar K, Yadav DB, Zuchero JY, et al. Mathematical PKPD and safety model of bispecific TfR/BACE1 antibodies for the optimization of antibody uptake in brain. *Eur J Pharm Biopharm*. 2016;101:53-61.
57. Betts A, Haddish-Berhane N, Shah DK, et al. A translational quantitative systems pharmacology model for CD3 bispecific molecules: application to quantify T cell-mediated tumor cell killing by P-Cadherin LP DART((R)). *AAPS J*. 2019;21(4):66.
58. Campagne O, Delmas A, Fouliard S, et al. Integrated pharmacokinetic/pharmacodynamic model of a bispecific CD3xCD123 DART molecule in nonhuman primates: evaluation of activity and impact of immunogenicity. *Clin Cancer Res*. 2018;24(11):2631-2641.
59. Leipold D, Prabhu S. Pharmacokinetic and pharmacodynamic considerations in the design of therapeutic antibodies. *Clin Transl Sci*. 2019;12(2):130-139.
60. Datta-Mannan A, Witcher DR, Tang Y, et al. Monoclonal antibody clearance. Impact of modulating the interaction of IgG with the neonatal Fc receptor. *J Biol Chem*. 2007;282(3):1709-1717.
61. Hayakawa M, Kushimoto S, Watanabe E, et al. Pharmacokinetics of recombinant human soluble thrombomodulin in disseminated intravascular coagulation patients with acute renal dysfunction. *Thromb Haemost*. 2017;117(5):851-859.
62. Shah DK, Betts AM. Towards a platform PBPK model to characterize the plasma and tissue disposition of monoclonal antibodies in preclinical species and human. *J Pharmacokinet Pharmacodyn*. 2012;39(1):67-86.

SUPPORTING INFORMATION

Additional Supporting Information may be found online in the Supporting Information section.

How to cite this article: Kiseleva RY, Glassman PG, LeForte KM, et al. Bivalent engagement of endothelial surface antigens is critical to prolonged surface targeting and protein delivery in vivo. *The FASEB Journal*. 2020;34:11577–11593. https://doi.org/10.1096/fj.201902515RR